

REPORT DOCUMENTATION PAGE

AD-A198 243

ELECTE

AUG 22 1988

1b. RESTRICTIVE MARKINGS

NA

3. DISTRIBUTION/AVAILABILITY OF REPORT

Unlimited

2b. DECLASSIFICATION/DOWNGRADING SCHEDULE

4. PERFORMING ORGANIZATION REPORT NUMBER(S)

H

5. MONITORING ORGANIZATION REPORT NUMBER(S)

NA

6a. NAME OF PERFORMING ORGANIZATION

Midwest Bio-Laser Institute

6b. OFFICE SYMBOL

(If applicable)

NA

7a. NAME OF MONITORING ORGANIZATION

Office of Naval Research

6c. ADDRESS (City, State, and ZIP Code)

4500 North Winchester Ave. Suite 508
Chicago, IL 60640

7b. ADDRESS (City, State, and ZIP Code)

800 N. Quincy Street
Arlington, VA 22217-50008a. NAME OF FUNDING/SPONSORING
ORGANIZATION Strategic
Defense Initiative Organization8b. OFFICE SYMBOL
(If applicable)

9. PROCUREMENT INSTRUMENT IDENTIFICATION NUMBER

N00014-86-K-0193

8c. ADDRESS (City, State, and ZIP Code)

Washington, D.C. 20301-7100

10. SOURCE OF FUNDING NUMBERS

PROGRAM
ELEMENT NO.
63222CPROJECT
NO.TASK
NO.

SDRP-007

WORK UNIT
ACCESSION NO.

11. TITLE (Include Security Classification)

(U) Midwest Free Electron Laser Program

12. PERSONAL AUTHOR(S) L.J. Cerullo, M.D.; M. Epstein, Ph.D.; M.E. Marhic, Ph.D.; W.Z. Rymer, M.D.,
Ph.D.; K.G. Spears, Ph.D. (all of Northwestern University); L.I. Grossweiner, Ph.D. (IIT)13a. TYPE OF REPORT
Annual

13b. TIME COVERED

FROM 3/1/87 TO 6/15/88

14. DATE OF REPORT (Year, Month, Day)

July 31, 1988

15. PAGE COUNT

14

16. SUPPLEMENTARY NOTATION

17. COSATI CODES

FIELD	GROUP	SUB-GROUP

18. SUBJECT TERMS (Continue on reverse if necessary and identify by block number)

Laser effects on neural tissue; Infrared picosecond laser;
Optical waveguides; Laser-tissue interactions; Neurosurgery;
Chrono-coherent imaging.

19. ABSTRACT (Continue on reverse if necessary and identify by block number)

► Subablative effects of pulsed Nd:YAG laser (1064nm) on the transmission of neural impulses in spinal cord dorsal white matter, spinal dorsal roots, and peripheral nerve in anesthetized rat were compared. The results to date indicate that long lasting impairment in both spinal synaptic transmission and small fiber input may be mediated by laser irradiation.

Nonlinear crystal mixing techniques have been employed to generate tunable infrared laser radiation in the 5-7 micron region with duration of 20ps. Characterization techniques of laser beams from the infrared to the ultraviolet were established for probing energy absorption and relaxation processes. Molecular studies of laser energy absorption and relaxation with relevance to fundamental studies in medicine and neuroscience were initiated. New methods to probe biological tissue with the FEL by spectroscopic or imaging techniques were developed.

New fabrication techniques of the whispering-gallery waveguide have been employed to obtain high quality specimens. Needle-like hollow metallic IR waveguides have been fabricated with
-over-

20. DISTRIBUTION/AVAILABILITY OF ABSTRACT

☒ UNCLASSIFIED/UNLIMITED ☐ SAME AS RPT ☐ DTIC USERS

21. ABSTRACT SECURITY CLASSIFICATION

Unclassified

22a. NAME OF RESPONSIBLE INDIVIDUAL
Dr. M. Marron22b. TELEPHONE (Include Area Code)
(202) 696-403822c. OFFICE SYMBOL
ONR

DD FORM 1473, 84 MAR

83 APR edition may be used until exhausted
All other editions are obsolete

SECURITY CLASSIFICATION OF THIS PAGE

DISTRIBUTION STATEMENT A

Approved for public release;
Distribution Unlimited

19. ABSTRACT (Continued)

lengths up to 30cm.

A diffuse optics spectrophotometer has been constructed that measures the optical constants of light scattering layers from 450 to 1350nm. Data analysis based on the diffusion approximation leads to values of the microscopic optical constants. The instrument has been employed in the measurements of endogeneous and exogeneous chromophore absorptions in tissue models and in vitro plant and animal tissues.

Accession For	
NTIS GRA&I	<input checked="" type="checkbox"/>
DTIC TAB	<input type="checkbox"/>
Unannounced	<input type="checkbox"/>
Justification	
By _____	
Distribution/	
Availability Codes	
Dist	Avail and/or Special
A-1	

MIDWEST FREE-ELECTRON LASER PROGRAM

ANNUAL REPORT: Contract N00014-86-K-0188

March 1, 1987 - June 15, 1988

I. Introduction

The Midwest Free-Electron Laser Program is managed by the Midwest Bio-Laser Institute, 4500 N. Winchester Avenue, Suite 508, Chicago, Illinois 60640, Tel. (312) 728-3828. The various research projects are conducted at the Technological Institute and the Department of Chemistry at Northwestern University in Evanston, Illinois; the Department of Physiology at Northwestern University Medical School in Chicago, Illinois; Department of Physics at the Illinois Institute of Technology, Chicago, Illinois; and the Wenske Laser Center of Ravenswood Hospital Medical Center, Chicago, Illinois. The management team consists of L.J. Cerullo, M.D., Program Director; M. Epstein, Ph.D., Program Administrator; L.I. Grossweiner, Ph.D., P.I. at IIT and Wenske Laser Center; M.E. Marhic, Ph.D., P.I. at NU's Technological Institute; W.Z. Rymer, M.D., Ph.D., P.I. at NU's Medical School; and K.G. Spears, Ph.D., P.I. at NU's Chemistry Dept. In addition to their duties as Principal Investigators of their individual projects, all of the above individuals participate in the management of the entire program, thus, assuring its unified and cohesive conduct. This is of particular significance, since the various projects are interdependent, being concerned with clinical studies of laser effects in neurosurgery, laser delivery systems, interactions of laser radiation with tissue and design of new laser systems.

The following are the progress reports of the individual research projects.

II. Laser Effects on Neural Tissue

P.I.: W. Zev Rymer, M.D., Ph.D., Dept. of Physiology, Northwestern University Medical School.

PROJECTS

1. Effects of Irradiation With Q-Switched Nd:YAG Laser Light on Dorsal Column White Matter in the Rat.

This study was designed to evaluate electrophysiological, thermal and histological effects of laser irradiation on neural tissue, concentrating on spinal cord dorsal column white matter of the rat. We chose dorsal column white matter because it contains a range of nerve fibers arranged in a parallel and orderly array in the long axis of the spinal cord, allowing application of relatively uniform laser irradiation. The sensory fibers of the dorsal columns are of varying diameter ranging from large, rapidly conducting fibers (diameter: 9-15 μm) to thin myelinated slower conducting fibers with smaller diameter ($< 3 \mu\text{m}$). These fibers come from a variety of different specialized receptors in muscles, skin, joints and viscera and display a broad range of biochemical and metabolic characteristics, making them interesting potential candidates to study novel photothermal and photochemical laser effects. We used Q-switched Nd:YAG laser light at 1064 nm wavelength with pulse energies from 10 to 100 mJ/pulse. At this wavelength radiation penetrates biological tissue for several millimeters, because of weak absorption by water and high scattering.

We studied the effect of irradiation with Q-switched Nd:YAG laser light on spinal cord

88 8 19 037

dorsal column white matter in 14 anesthetized rats. To evoke a synchronous sensory input the sciatic nerve was stimulated electrically at supramaximal intensities and the resulting evoked spinal cord potential (SCP) was recorded from the dorsal columns of the ipsilateral side with low impedance glass microelectrodes. The wave shape of the SCP showed three components: an early positive peak (P1), representing the responses of the most rapidly conducting fibers, followed by two negative peaks (N1 and N2), which are due to synaptic effects of small afferent fibers on dorsal horn cells located in dorsal grey matter.

Nd:YAG laser irradiation for 5 min each at pulses with increasing energies caused a progressive but non-uniform decrease in the amplitude of each of the peaks, beginning at laser energies of 50 mJ/pulse. Laser irradiation at this energy level and above resulted in *severe reduction in the amplitudes of N1 and N2, with little or no reduction in the amplitude of P1.* This effect of Q-switched Nd:YAG laser irradiation on the amplitudes of N1 and N2 was partly reversible over time. However, when pulse energies above 80 mJ/pulse were used, changes in amplitude were more longlasting.

The observed effect of Nd:YAG laser irradiation on the synaptically mediated slow components of the spinal cord potential versus the fast component, mediated through fast conducting fibers, could either be caused by photothermal or photochemical laser effects. Since the mean temperature measured in the spinal cord 0.5 to 1 mm below the area of irradiation was above 60 °C, a level known to cause denaturation and coagulation, it is likely that the observed electrophysiological alterations were thermally mediated. Histological studies on the lightmicroscopic level showed that the electrophysiological changes at laser irradiations of 50 to 70 mJ/pulse were not accompanied by obvious tissue disruption.

The selective loss of the synaptic field could be mediated by loss of small fiber input to the dorsal horn or by impairment of synaptic transmission

2. Effects of Irradiation With Q-Switched Nd:YAG Laser Light on Dorsal Root Compound Action Potentials

Our previous study on laser effects on dorsal column white matter had shown that irradiation with Q-switched Nd:YAG laser light selectively reduced the synaptically mediated component of the evoked spinal cord potential. This study was designed to further investigate the mechanism responsible for the selective loss of the synaptic field.

All fibers travelling in the dorsal columns of the spinal cord reach the cord from the periphery via the dorsal roots. In this study we evaluated electrophysiological effects of laser irradiation on the compound action potentials in dorsal roots L4 and L5 evoked by supramaximal electrical stimulation of the ipsilateral sciatic nerve in the rat (7 experiments). The electrically evoked compound action potential usually consisted of a positive asymmetrical wave with two peaks. Laser irradiation (duration: 5 min) at 20 mJ/pulse and above caused a progressive reduction of the late portion of the compound action potential, implying a differential effect of Q-switched Nd:YAG laser irradiation on slow versus fast conducting fibers in dorsal roots. It might be possible that this preferential effect of laser irradiation on small fibers was due to high temperatures as they occur during laser application. Because of the smaller heat sink effect provided by the narrower cross-sectional area in small fibers it is likely that the intraaxonal temperature reaches a disproportional higher level in small diameter fibers than occurs in larger diameter fibers.

Since the data of this study showed that laser irradiation caused a preferential impairment of slow conducting fibers in dorsal roots it might be possible that the observed loss of the synaptic field in the spinal cord (exp. series 1, see above) is due to loss of slow fiber input to dorsal horn neurones.

3. Effects of Irradiation With Q-Switched Nd:YAG Laser Light on Sciatic Nerve Compound Action Potentials

Dorsal root compound action potentials show an asymmetrical waveshape, which varies substantially between animals. This is probably due to variations in the number of afferent fibers of each class entering each dorsal root. Therefore we decided to repeat the experiment using a compound action potential with a more symmetrical waveshape and less inter animal variability.

We used the compound action potential recorded from the sciatic nerve after supramaximal electrical stimulation of the tibial nerve. Experiments were performed on 13 anesthetized rats. Laser irradiation at increasing pulse energies caused a progressive reduction of the late portion of the sciatic nerve compound action potential, resembling the laser effects observed in dorsal root compound action potentials.

This study confirms our previous observation that Q-switched Nd:YAG laser irradiation preferentially impairs slow conducting fibers as compared to fast conducting fibers.

4. A Model to Describe the Effect of Laser Irradiation on Conduction Velocity Distributions in the Sciatic Nerve of the Rat

This study was designed to give a quantitative estimate of the changes in the relative conduction velocity distributions during laser irradiation of the sciatic nerve.

Conduction velocity distributions before, during and after laser application were calculated using the compound electrical nerve response recorded in response to supramaximal stimulation and an estimate of the single fiber response based on threshold stimulation (Cummins, Kovacs and Barker, 1981). Our data showed that during laser application the percentage of the relative distribution of slow conducting fibers was increased whereas the percentage of fast conducting fibers was decreased. Five minutes after laser irradiation conduction velocity distributions were almost equal to distributions before laser irradiation.

SUMMARY

Our studies have shown that Q-switched Nd:YAG laser irradiation of dorsal column white matter preferentially impairs the potential fields evoked primarily by synaptic effects of small afferent fibers on dorsal horn cells. Data from experiments on dorsal roots and sciatic nerves imply that irradiation with laser light has differential impact on slow versus fast conducting fibers. Our present hypothesis is that the observed loss of the synaptic field in the spinal cord could be due to loss of small fiber input to dorsal horn cells. It is likely that these effects are thermally mediated, because temperatures recorded during laser irradiation were substantial.

III. Infrared Picosecond Laser Development and Applications

PI : Kenneth G. Spears, Ph.D., Depts. of Chemistry and Biomedical Engineering, Northwestern University.

Objectives:

1. Complete development of a laser system for simulating the picosecond pulse duration, energy and wavelengths of a free electron laser (FEL).
2. Characterize the laser outputs and set up experiments for probing energy absorption and relaxation processes with wavelengths from the infrared to the ultraviolet.
3. Initiate molecular studies of laser energy absorption and relaxation with relevance to fundamental studies of medicine and neuroscience.
4. Develop new methods to probe biological tissues with the FEL by spectroscopic or imaging techniques.
5. Set up new wavelength capabilities for a Nd-YAG pulsed laser which can be used in neuroscience research.

Accomplishments:

1. Picosecond Laser Development

The method developed last year for tunable IR generation was refined and extended into new wavelength regions. We used nonlinear crystal mixing techniques to generate tunable infrared wavelengths in the 5-7 μm region with durations of 20 ps. The amplification of 1 ps dye laser pulses was briefly tested to establish the synchronization of the 10 Hz Nd:YAG laser and the CW mode-locked dye laser. These pulses will require additional development of another 1 or 2 stages of gain to be used with the infrared crystal mixing technique. Our plans in the next year are to do some of the experiments requiring such pulses at an FEL site, and do the development work when the FEL is not available. The laser system at 20 ps duration was reliable, and it was heavily used in experiments during the last year. The new technique of generating infrared laser radiation was accepted for publication in Optics Communications.

2. Laser Characterization and Experimental Setup

The tunable dye laser and 532 nm harmonic of the Nd:YAG laser were studied with two methods to determine the coherence time of the pulses. A four wave mixing method and a very simple interference method on holographic grade film were compared. The dye laser coherence time of 2 ps is much shorter than its duration of 20 ps, while the 532 nm pulse is 8 ps in coherence time compared to 25 ps in duration. The technique of using film is currently being theoretically compared to four wave mixing, and will soon be prepared for publication.

The pump-probe geometry using infrared probes was set up for studies of energy relaxation by molecules. This method requires that a pump beam at some wavelength from the IR to the UV be overlapped with a probe beam in the infrared, while quantitative measurement of the pump, the probe, and a reference for the probe be made on each shot of the laser. The requisite optics, detectors, and computer control were all accomplished and tested on actual systems.

3. Molecular Studies

The objectives of our initial experiments were: 1. Study electron transfer processes and their environmental effects due to charge formation, 2. Study a protein electron transfer system to determine conformational and geometry parameters of electron transfer, and 3. Study a photodissociating molecule where the tunable infrared can be used to monitor specific molecular fragments.

The solvent dependence of charge formation was studied by an intramolecular dissociative electron transfer process. A neutral molecule was selected which can transfer an electron internally to form a small anion (cyanide or hydroxyl) and a triphenylmethyl cation (positive charged). This process is very dependent on the molecular environment, and we have elaborated how this dependence correlates with molecular dielectric properties and local solvent configurations around the molecule. This work has shown how an ionic transition state interacts with the solvent, where configurations (or entropy) are more important than energy. This type of molecule may be a very good probe of membrane environments and we will explore its use in models of neurotransmitter vesicle membranes. The results are currently being written for publication.

The second system for electron transfer studies is the cytochrome c protein. The research groups of Prof. B. Hoffman and E. Margoliash of Northwestern University have pioneered the study of electron transfer between cytochrome c and an oxidase protein. We have begun a collaboration with these groups, and have made some measurements of energy transfer between the two proteins in their "docked" complex. The purpose is to identify the geometry and conformational changes resulting from temperature changes and genetic mutation changes in the cytochrome c partner. These data are obtained by picosecond energy transfer measurements with fluorescence quenching methods. Our preliminary results show significant effects from single mutations in the protein, and more work is proceeding to demonstrate the temperature effects. These studies will be complementary to future electron transfer measurements, and, we hope, will give some new definition to biological processes. Such work ultimately may relate to photo-induced processes in cells.

The third system was designed to understand how dissociating molecules can be studied with a tunable infrared laser source. We have studied the UV wavelength excited state dissociation of $\text{Cr}(\text{CO})_6$ to eject one and two CO molecules. The IR probe laser could probe the specific fragments and their reaction with solvent molecules. In addition, vibrational excitation of the fragments could be measured. Preliminary results show that one CO ejection is much more probable than two, and the fragment from one CO ejection is left vibrationally excited while the case of two CO ejection has little vibrational excitation. These results are significant demonstrations of how to monitor molecular changes from high power laser pumping of molecules. We will soon finish this calibration study and move on to biologically related systems, especially neurotransmitter molecules.

4. New Spectroscopic and Medical Imaging Techniques

Our use of laser techniques for spectroscopy have been extended to develop a new method for medical imaging. We have worked with Professor Nils Abramson of Sweden in our laboratory in order to define the possibility of adapting his light-in-flight measurement method to medical imaging. We have performed a demonstration experiment and several recent tests of dynamic

range which suggest that a totally new and revolutionary medical diagnostic method can be developed. We have called this method Chrono-Coherent Imaging (CCI).

The problem of viewing inside the human body is fundamentally related to the light scattering and absorption properties of tissue. There are many wavelengths in the near infrared which can transmit through a tissue such as the breast, but the light scattering leaves only very diffuse image content after transmission and, thus, has limited applications. A coherent image formation process, however, requires an interference of the reference beam and the object beam to form an image which needs reconstruction by a coherent laser. Such image formation when done with pulses of coherence length much larger than the object size leads to holographic image formation. However, the short duration of a picosecond coherence time can create an image over a sequence of times where a specific time delay from a reflected object pulse relates to a specific depth position of the object (like two dimensional slices). This light-in-flight reflection technique can be adapted to a transmission geometry where time delay of scattered light does not show up in phase with the reference beam, while the absorbing or time delay properties of the media can make a coherent image. In this CCI method we essentially discriminate against the media scattering because these scattered rays take different time delays to arrive at the recording medium. The dynamic range of holographic media is such that very weak transmitted beams which form coherent images can be detected in the presence of strong scattered light exposure which is not coherent. Our recent tests have established that many orders of magnitude more intense scattered light than coherent object light can be present and still yield a useful image. In the future, we expect that CCI can become an important medical diagnostic method. The FEL can be used in the near infrared to give good spatial resolution and selectivity of tissue imaging inside tissues such as breast, arm, etc. We expect this method to be useful in cancer screening and other diagnostic applications. The first paper is being prepared and others will soon follow.

5. Laser for Neuroscience Research

We have received a pair of Raman shifter cells for 1.54 and 1.91 μm wavelengths which were designed for compact, efficient use with a 1.06 μm pump laser. We will soon complete tests of their efficiency with three laser sources: the 8 ns laser that is used for neuroscience research, the picosecond 10 Hz Nd:YAG laser, and a Q-switched, mode-locked CW Nd:YAG laser. We will soon install these Raman shifting cells in Professor Rymer's laboratory for work on the neuroscience project with the 8 ns pulse Nd:YAG laser.

IV. Infrared Waveguide for Laser-Beam Delivery

P.I.: Michel E. Marhic, Ph.D., Dept. of Electrical Engineering and Computer Science, Technological Institute, Northwestern University

1. Whispering-gallery (WG) guides.

We have calculated, using two different approaches, the contribution of the second curvature to the losses and found that, at the wavelength of 10 μm , losses for a gold-coated guide should be on the order of 2 percent per turn. These numbers hold for the fundamental mode, and increase slowly with mode number. Thus, low-loss propagation is attainable if only the fundamental, or a few low-order modes, are excited by proper alignment. We have also performed calculations to find the increase in loss due to stretching of the structure into a helical shape, which introduces torsion (τ) of the ray trajectories, and found that the influence of τ on the losses should remain moderate provided that reasonable deformations of the guides are used. Employing accurate methods of analysis to study the off-axis oscillations it was determined that

the increase in loss due to the kinds of oscillations often observed in practice is essentially negligible.

We evaluated the use of overcoating the metal with one or more dielectric layers. Most benefits are derived in the case of a double quarter-wave layer (designed to operate at or near a single frequency). This structure can be thought of as an impedance transformer, increasing the metal impedance by a factor of $(n_1/n_2)^2$, where n_1 and n_2 are the indices of refraction of the two layers. By choosing a pair of high and low index materials, such as Germanium and Lithium Fluoride, the TE losses can, in principle, be reduced by nearly an order of magnitude below the bare-metal value, to something on the order of 0.3 percent per turn. A difficulty for FELs is that such structures are resonant, being optimized for a single wavelength; thus they would not be useful over the entire wide range anticipated for some FELs.

We sought to develop better methods of fabrication of the WG guides and chose to make them by electroforming. We start with constructing an aluminum mandrel which goes through stages of buffing, lap polishing, and nickel plating, in order to produce a defect-free mirror-like surface. We then overcoat it with a thin layer of gold in our vapor deposition chamber, and build a thick nickel wall over the gold by electroplating. The nickel-gold structure is then separated from the mandrel, thus yielding a self-supporting WG guide, with a mirror-like gold-coated inner surface.

The results obtained to date with the electroformed guides are somewhat disappointing in that the losses are stubbornly pegged at about 6 percent per turn, which is still about three times higher than theoretically possible. We have identified several possible causes of this discrepancy and are in the process of modifying the fabrication techniques to approach theoretically predicted values. These include improved vapor and sputtering deposition and thin film diagnostic and monitoring.

Over the past year we have performed a number of experimental studies on the WG guides, the highlights of which are summarized below.

- a. Average power. We have tested our WG guides with a CO₂ laser operating near 10 μm , with an output power of 80 Watts. Temperature rise was measured, and found to be of the order of 10 $^{\circ}\text{C}$, without any cooling; no local damage was noticed on the inside of the guide. It would appear that the guides could transmit more power at this wavelength, or the same power at shorter wavelengths without any ill effects.
- b. Peak power. We have performed peak-power tests using an infrared laser system with peak power in the megawatt range, and have observed no degradation in performance.
- c. Losses vs. wavelength. The laser system used in b is based on a Nd:YAG oscillator, used to generate tunable IR radiation in the 1 to 10 μm range, to simulate the tunability of an FEL. As expected, we have found that the losses are lowest at 10 μm (6 % per turn), and highest at 1 μm (15 % per turn), with a monotonic variation in between. Also, measurements performed with a He-Ne laser at 0.63 μm yielded about 20 % loss per turn. The increase at short wavelengths results in part from the decreased index of refraction, as well as from increased scattering from surface roughness (which looks relatively larger at short wavelengths).
- d. Tests in FIR. Although we are primarily interested in developing WG guides for the 1 to

10 μm range, we note that these hollow metallic guides could also be useful at longer wavelengths, such as in the far-infrared, where some FELs are also available. Preliminary measurements indicate surprisingly high losses at 400 μm . These may come from a number of extraneous sources such as absorption of FIR radiation in air, extra losses due to rapid diffraction and difficulty to focus the FIR into the guide and the detector.

We have studied the behavior of the WG guides under deformations. Since the WG guides are meant to be flexible, it is desirable that their losses remain low under a variety of deformations. We have verified this experimentally and have found that, for our best unit, losses per turn rose from 6 to 7 percent by going from a compressed configuration to one where a stretched helix is obtained, making an angle of about 30 degrees with its axis. This corresponds to a large deformation, useful in practical situations, and so this measurement indicates that the WG guides can be stretched in a practical manner without an appreciable increase in loss. We have also subjected the WG guide to more general deformations. In particular, we have induced, what might be called, an "accordion" deformation, whereby the coil is stretched from its compressed position, but more so on one side than on the other; the result is that the overall coil shape lies on a torus (rather than on a straight circular cylinder when stretched into a helix). We have induced rather extreme accordion deformations, keeping one side of the coil compressed, and opening the other side widely, and again noted very little increase in loss.

These measurements indicate that WG guides can withstand rather substantial deformations from their compressed state, without exhibiting very large increases in loss. This confirms that they should be useful in a variety of practical situations where they may be subjected to a variety of arbitrary deformations, similar to the ones tested experimentally.

2. Hollow circular guides.

These needle-like waveguides have much in common with the WG guides, in that they are hollow metallic guides, also made by electroforming. Since the theory of losses in such guides is rather well understood, we have not spent much time on theory, but rather concentrated on fabrication.

Although we have explored the use of soluble glass and silica tubes to fabricate the required mandrels, we are, at the present time, still utilizing aluminum mandrels. To improve the surface conditions of extruded tubes, we have them ground centerless to remove extrusion defects. These tubes are then dissolved using KOH or NaOH, which are relatively harmless chemicals.

The mandrels are coated with a gold layer, much as the WG guides. We have developed a special apparatus to allow for the coating of a large number of specimens in order to eliminate the waste of expensive gold coating. The ID of current tubes is 1.5 mm, but could eventually be made smaller, particularly if silica mandrels are used.

The gold-coated mandrels are overcoated by electroforming with a thick nickel wall, as described in the case of the WG guides. The mandrel is then dissolved by circulating the appropriate solvent through it. This leaves a self-supporting nickel guide, with a smooth gold surface on the inside.

So far, we have tested short straight guides only, and they have exhibited low losses, as expected. The real tests will take place when we use longer tubes and bend them. In that case

the losses of metal-coated guides will increase rapidly, and we will have to resort to dielectric coatings in order keep them low.

We have initiated, in collaboration with Dr. L. Cerrulo, Director of the Midwest FEL Program, and his colleagues at the Chicago Institute for Neurosurgery and Neuroresearch (CINN), the development of novel designs utilizing hollow waveguide structures. In particular, in collaboration with Dr. Helenowsky of CINN, we are attempting to design a CO₂ laser beam delivery system to be used in brain surgery, such as extension or replacement of the articulated arm and curved hand-pieces, which will overcome the limitations of currently used devices.

V. Interaction of Laser Radiation with Tissue

P.I.: Leonard I. Grossweiner, Ph.D., Physics Department, Illinois Institute of Technology.

INTRODUCTION

Essentially all phenomena in photomedicine involve light interactions with chromophores embedded in tissue. The initial effect may be a photochemical reaction, light emission, or heat generation, depending on the specific chromophore, the microenvironment, and the wavelength. The light scattering properties of tissues preclude the use of ordinary spectroscopic techniques for the investigation and analysis of these phenomena. This project emphasizes the development and applications of tissue optics methods for the study of laser interactions with model tissues.

SUMMARY OF RESULTS

1. Measurement and Analysis of Tissue Optical Constants

A two-channel diffuse reflectance spectrophotometer was designed and constructed for the measurement of total transmission (T_t) and diffuse reflection (R_d) from 450 to 1350 nm. The system utilizes 10 cm integrating spheres illuminated with chopped monochromatic light. The isotropic radiant flux within each sphere is coupled to either a red-sensitive photomultiplier or a germanium diode, measured with a lock-in amplifier, and read into microcomputer. A typical run leads to values of R_d and T_t for a given sample at 5 or 10 nm intervals.

The optical constants are calculated with a FORTRAN program based on the one-dimensional diffusion approximation (1DA), using the algorithms kindly provided by Dr. S. L. Jacques of Harvard Medical School. The program searches for values of the absorption coefficient (k) and scattering coefficient (s) for specified values of the anisotropy coefficient (g) and internal total reflectance coefficients (r_i). Alternatively, the experimental value of the $1/e$ penetration depth (δ) can be specified, and the program searches for k , s , and g .

Figure 1 shows a plot of k vs wavelength for bovine muscle. The calculation was based on the "similarity principle", with $g = 0$ and $s' = s(1 - g)$. The myoglobin absorption peaks at 542 nm and 578 nm are clearly visible. The oscillations above 850 nm are overtones of the water bands. A search for g at 1064 nm led to $g = 0.65$, based on the experimental value $\delta = 3.28$ mm measured with the heat pulse method (see below). Figure 2 shows the true absorption spectrum of sweet potato tuber incubated in Photofrin II. The absorptions below 550 nm are carotenoid pigments. The two longest wavelength porphyrin absorptions are clearly resolved.

In present work, the photodynamic inactivation of the endogenous enzyme β -amylase in sweet potato is being investigated with Photofrin II as the photosensitizer. This model system includes the key components of photodynamic tumor therapy (PDT) at the molecular level: a light scattering tissue with intrinsic absorption, the photosensitizer, and a singlet-oxygen sensitive biological target.

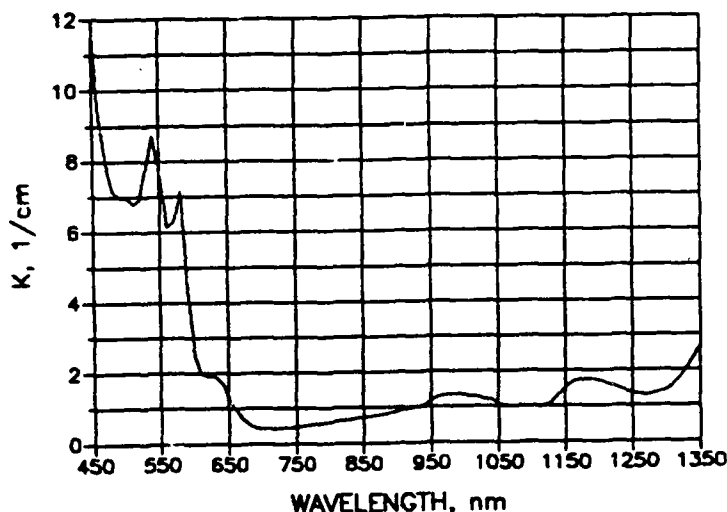


Figure 1. Absorption coefficient of bovine muscle calculated with one-dimensional diffusion approximation from experimental values of diffuse reflectance and total transmission.

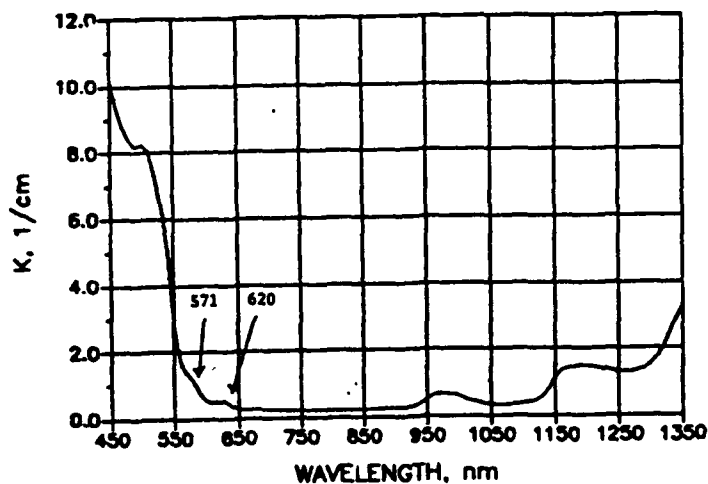


Figure 2. Absorption coefficient of sweet potato tuber incubated in Photofrin II.

2. Polystyrene Microsphere Tissue Models

Various animal and plant tissues have been used for measurements of tissue optical properties. However, *in vitro* tissues may not be convenient for studies of photosensitized processes because they lack an appropriate biological target. Prior work in this laboratory has

shown that aqueous suspensions of polystyrene microspheres with methylene blue as an absorber and subtilisin Carlsberg as the biological target can be employed as tissue models. [L. I. Grossweiner and J. W. Messina, "Investigation of power absorption by methylene blue in a light scattering medium with an internal photodynamic actinometer." *Photochem. Photobiol.* **45**, 617-624, 1987]. Since k is known, s' can be calculated by measuring a single optical property such as δ . The linear dependence of s' on the microsphere concentration leads to g , where s is calculated with Mie scattering theory. The optical constants also permit the calculation of the radiant energy fluence rate (ϕ) within the layer. The energy absorption rate obtains by integrating $k\phi(x)$ over the layer. The present study extends the prior work by employing Photofrin II (PFII) as the photosensitizer and measuring the photodynamic inactivation of subtilisin Carlsberg with red and green light. The photochemical rate constants (κ) were compared to the predictions of 1DA utilizing the measured optical constants.

Measurements were made at 633 nm and 546 nm for 2 μ m polystyrene microspheres in 1:150 Photofrin II with 1% Triton X-100 to suppress aggregation of the porphyrins. The $\phi(x)$ profiles measured with a 2 mm spherical tip fiber optic probe were accurately exponential for more than one decade, leading directly to values of δ . For microsphere concentrations from 1×10^7 to $5 \times 10^8/\text{cm}^3$, the calculated value of $s(1 - g)$ was $2.48 \times 10^{-8} \text{ cm}^2$ at 633 nm and $8.68 \times 10^{-9} \text{ cm}^2$ at 546 nm. A comparison with more strongly absorbing "India Ink" at 633 nm led to $s(1 - g) = 2.55 \times 10^{-8} \text{ cm}^2$. The Mie scattering cross sections for non-absorbing 2 μ m diameter spheres are 10.04×10^{-8} and $7.86 \times 10^{-8} \text{ cm}^2$, at 633 and 546 nm, respectively, leading to $g = 0.75$ at 633 nm and $g = 0.89$ at 546 nm. The correct magnitude g obtained by this indirect approach supports the validity of 1DA for the microsphere systems.

The same systems were irradiated at 546 nm and with red light (590-640 nm) in the presence of subtilisin Carlsberg, and the rate of energy absorption was calculated from the rate of photodynamic inactivation (κ). The key results are:

- (a) The value of κ was almost constant at each irradiation wavelength where δ at different microsphere concentrations varied from 0.4-0.9 cm. This result is supported by 1DA calculations showing that higher scatterer concentrations increase R_d and decrease T_t , while the integrated fractional absorption remains relatively constant for a given k .
- (b) The photodynamic rate constant corrected for the incident irradiance was approximately 3-fold higher with green light than red light. This result suggests that green light PDT might be advantageous for thin tumors, such as carcinoma *in situ* in an epithelial membrane, in order to achieve higher light doses or shorten the treatment time.

3. Tissue Heating with Pulsed Nd:YAG Laser

The basic physics of laser-tissue interactions indicates that thermal damage to peripheral tissues can be confined by using sufficiently short pulses. In continuous mode (CW) operation, heat flow driven by temperature gradients leads to tissue heating external to the optical absorption profile. When the energy is delivered in pulses, however, conductive heat flow is minimized if the pulse duration (t_p) is shorter than the thermal relaxation time constant (t^*). Pulsed operation should be especially useful for the Nd:YAG laser, where δ at 1064 nm is the order of 0.3 to 0.5 cm. Taking $t^* = \delta^2/2\alpha$, where α is the thermal diffusivity (the order of $0.001 \text{ cm}^2/\text{s}$ for tissues), typical values of t^* for heat conduction are the order of 1-2 min. Heat removal by blood flow augments thermal conduction in vascularized tissues. The rate of this

process is characterized by $1/Q$, where Q is the volume blood perfusion rate. Values $1/Q$ range from the order of 15 s for human kidney and thyroid to more than 15 min for muscle (Svaasand, 1982). Accordingly, heat removal by conduction and blood flow during the pulse duration can be neglected for many tissues exposed to Nd:YAG laser pulses. An analytical solution to the two dimensional laser bioheat equation has been obtained for pulsed operation. The analysis was compared to measurements on potato tuber and bovine muscle heated by pulses from a clinical Nd:YAG laser. The laser bioheat equation for radial symmetry without an internal heat source was solved for rectangular and gaussian beam profiles using the method of Fourier integrals. The solution has the form:

$$T(r,x,t) = F(x,t)S(r,t) \quad (1)$$

where:

$$F(x,t) = (1/2)\text{Exp}(\alpha t/\delta^2) \{ \text{Exp}(x/\delta)\text{Erfc}[\sqrt{\alpha t}/\delta + x/2\sqrt{\alpha t}] + \text{Exp}(-x/\delta)\text{Erfc}[\sqrt{\alpha t}/\delta - x/2\sqrt{\alpha t}] \} \quad (2)$$

where α is the thermal diffusivity.

The solution for S with a gaussian profile is:

$$S_g(r,t) = \frac{K_g \text{Exp}\{-r^2/[b^2(1 + 4\alpha t/b^2)]\}}{(1 + 4\alpha t/b^2)} \quad (3)$$

A rectangular profile gives a complicated equation for S that must be integrated numerically, which reduces to a simple result at the spot center:

$$S_r(0,t) = K_r[1 - \text{Exp}(-r_0^2/4\alpha t)]. \quad (4)$$

The evaluation of K requires optical and thermal parameters for the specific tissue. The initial temperature rise immediately after the pulse is given by the heat balance:

$$\rho C T(x,r,t_p) = U(x,r) k t_p \quad (5)$$

where ρ is the tissue density and C is the tissue specific heat. For a semi-infinite layer the K functions are:

$$K_g = (P t_p / \pi \delta b^2 \rho C)(1 - R_d) \quad (6a)$$

$$K_r = (P t_p / \pi \delta r_0^2 \rho C)(1 - R_d) \quad (6b)$$

where P is the pulse power and t_p is the pulse duration. The analysis utilizes values of $T(x,0,t)$ calculated with a FORTRAN 77 program based on Eqs. (1-6).

Approximately 5 cm cubes of Idaho potato tuber and bovine muscle were heated by single 0.3 s pulses from a Cooper LaserSonics Model 8000 Nd-YAG laser. The measurements were

carried out with an 8 mm diameter laser beam, to minimize the errors related to the neglect of beam spreading and inaccurate location of the thermocouple at the spot center. The temperature rise was measured on the beam axis at depths of 1 to 6 mm from the illuminated face, using unshielded 28 gauge copper-constantan thermocouples and copper-constantan thermocouple probes in a 30 gauge hypodermic needle. The thermocouple measurements were augmented by non-invasive surface temperature measurements with an infrared thermometer. The initial temperature elevation, corrected for thermocouple heating, was proportional to the product of P and t_p , for $t_p = 0.1 - 0.5$ s and $P = 10-80$ W, confirming that tissue cooling during the pulse duration was negligible. A novel thermal method was used to determine δ at 1064 nm by measuring the dependence of the initial temperature rise on depth.

(a) Idaho Potato Tuber

The water content was measured as $82 \pm 5\%$ by prolonged incubation at 105°C and weighing, and the specific density was measured as 1.25 ± 0.05 . General expressions for tissue thermal properties lead to $C = 3.7$ kJ/kg $^\circ\text{C}$ and $\alpha = 0.0011$ cm²/s. The value of δ obtained with the heat pulse method was 3.7 mm, based on the average of five experiments with 0.3 s pulses at 19.6 W. The diffuse reflectance of a thick Idaho potato slab was 0.37 at 1064 nm. The measured initial temperature elevations from 0-3 mm depth are in good agreement with the computer calculations. However, the rate of thermal relaxation was significantly faster than predicted. For example, t^* was 15 s at $x = 1$ mm, compared to the calculated value of 50 s. The rapid cooling cannot be attributed to the neglect of surface convection in the analysis. The surface temperature was unchanged when the irradiations were carried out in a 100% humidified atmosphere and when the tissue surface was cooled by forced air, providing additional support for the exclusion of surface convection as the cause of the fast relaxation. An alternative mechanism involves energy loss by evaporation of internal water, which is the only important absorber at 1064 nm. The required heat loss per pulse is accounted for by 1% evaporation of internal water. This effect may be more pronounced because radial heat flow was negligible for the 8 mm beam diameter.

(b) Bovine Muscle

Similar procedures were employed with bovine muscle. The heat pulse method led to $\delta = 3.28$ mm at 1064 nm, based on the average of ten experiments with thermocouples at 1-4 mm depth. The diffuse reflectance was measured for 15 samples of different thickness, which led to $k = 1.094 \pm 0.1832$ cm⁻¹ and $s(1-g) = 6.339 \pm 1.239$ cm⁻¹, and $R_d = 0.33$ for a thick sample. The thermal calculations are based on $\rho = 1.095$ g/cm³ (measured), $C = 3.47$ J/g $^\circ\text{C}$ (estimated), and $\alpha = 0.0012$ cm²/s (estimated). The calculated initial temperatures are about two-fold higher than measured. The rate of thermal relaxation was comparable to potato tuber and faster than predicted. When a sample was exposed to CW radiation at 5 W, the temperature build-up and relaxation times were approximately 50 s, as expected. This result indicates that the low values of t^* are characteristic of pulsed delivery, which is consistent with the hypothesis of fast evaporative heat loss. This work is being continued in order to identify the factors responsible for the differences between the calculated and measured temperature rise profiles.

VI. Publications

1. Wesselmann, U., S.-F. Lin and W. Z. Rymer, "Differential effects of irradiation with Q-switched Nd:YAG laser light on the components of the spinal cord potential evoked by electrical stimulation of the sciatic nerve in the rat". (full paper, submitted to *Brain Res.*).
2. Wesselmann, U., S.-F. Lin and W. Z. Rymer, "Effects of Nd:YAG laser irradiation on electrically evoked spinal cord potentials", (abstract, submitted to the *11th Annual Meeting of The European Neuroscience Association*, Zurich, Switzerland, 1988)
3. Wesselmann, U., S.-F. Lin and W. Z. Rymer, "Nd:YAG laser effects on compound action potentials of spinal cord, dorsal roots and the sciatic nerve in the rat ",(abstract, submitted to the *Annual Meeting of The Society For Neuroscience*, Toronto, Canada, 1988)
4. Lin, S.-F., "Laser Effects on Nervous Tissue", (thesis for a Masters Degree in Biomedical Engineering; in preparation)
5. Wesselmann, U., S.-F. Lin and W. Z. Rymer, "The influence of Nd:YAG laser light on compound action potentials of dorsal roots and sciatic nerves in rats", (manuscript in preparation).
6. Spears, K. G., X. Zhu, X. Yang and L. Wang, "Picosecond infrared generation from Nd-YAG and a visible, short cavity dye laser", *Optics Communications*, 1988, in press.
7. Jiao, J., W.L. Kath, X. Fang and M.E. Marhic, "Losses of infrared biconcave metallic whispering-gallery guides", *Fourth International Conference on Infrared Physics*, Zurich, Switzerland, August 22-26, 1988.
8. Kath, W.L., J. Jiao, X. Fang and M.E. Marhic, "Losses for vector solutions of infrared whispering-gallery waveguides", *Annual Meeting of the Society for Industrial and Applied Mathematics*, Minneapolis, MN, July 11-15, 1988.
9. Grossweiner, L.I., "Interactions of light with biological tissue", In *Photosensitization, Molecular, Cellular and Medical Aspects*, (Ed. G. Moreno, R. H. Pottier, and T. G. Truscott), Springer-Verlag, Berlin Heidelberg, 1987, pp. 101-110.
10. Karagiannes, J.L., and L. I. Grossweiner, "Optical measurements on tissue layers", In *Photosensitization, Molecular, Cellular and Medical Aspects*, (Ed. G. Moreno, R. H. Pottier, and T. G. Truscott), Springer-Verlag, Berlin Heidelberg, 1987, pp. 111-116.
11. Grossweiner, L.I., "Photosensitization in a light scattering medium", *2nd Congress of the European Society for Photobiology*, Padua, ITALY, September 6-10, 1987; Plenum Press, New York, in press.
12. Grossweiner, L.I., and A. M. Al-Karmi, "Tissue heating with a pulsed Nd-YAG laser", *SPIE O-E LASE '88*, Los Angeles, CA, January 10-17, 1988, *SPIE Proceedings*, in press.
13. Grossweiner, L.I., "Photosensitization in light scattering media", *American Society for Photobiology*, Colorado Springs, CO, March 13-17, 1988; *Photochem. Photobiol.* 47:19S, 1988.